Journal of Molecular Structure 975 (2010) 274–279

Contents lists available at ScienceDirect

Journal of Molecular Structure

journal homepage: www.elsevier.com/locate/molstruc

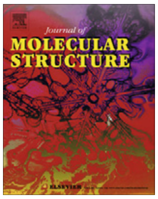

Directionality and site selectivity of N···Cl halogen bonding in two azaaromatic chloride crystals

Yi-Min Zhu [a], Ti-Fang Miao [a,b], Yang-Yi Yang [a,*], Dong-Yue Zhuang [a], Kang-Cheng Zheng [a], Wing-Tak Wong [c]

[a] MOE Key Laboratory of Bioinorganic and Synthetic Chemistry, School of Chemistry and Chemical Engineering, Sun Yat-Sen University, Guangzhou 510275, PR China
[b] College of Chemistry and Materials Science, Huaibei Normal University, Huaibei 235000, PR China
[c] Department of Applied Biology and Chemical Technology, The Hong Kong Polytechnic University, PR China

ARTICLE INFO

Article history:
Received 9 March 2010
Received in revised form 23 April 2010
Accepted 23 April 2010
Available online 29 April 2010

Keywords:
Halogen bonding
Directionality
Site selectivity
DFT calculations
Molecular electrostatic potential

ABSTRACT

Two azaaromatic chlorides of bis-2,4-[(2-formoyl)phenoxyl]-6-chloro-[1,3,5]triazine (**1**) and bis-2,4-(4-carbomethoxyphenoxyl)-6-chloro-[1,3,5]triazine (**2**) have been synthesized and structurally characterized. The crystal structures of **1** and **2** reveal unusually short intermolecular N···Cl distance of 3.095(2) and 3.088(3) Å, meaning the formation of strong halogen bonding. The strengths of the intermolecular N···Cl halogen bonding and the molecular electrostatic potentials in these crystal structures have been calculated by Density Functional Theory Calculations. The capacities of the N···Cl halogen bonding, lone pair···π interaction, π–π stack and C—H···O hydrogen bonding in the directionality of supramolecular self-assembly have been analyzed by structural study and theoretical calculations. The site selectivity of the N···Cl halogen bonding is illustrated by the difference of electrostatic potential of the N atoms on the molecule.

1. Introduction

Intermolecular interactions play crucial roles in supramolecular chemistry [1] and crystal engineering [2]. Among these interactions, hydrogen bonding and π–π stack are probably the most important ones [3,4]. Very recently, a new kind of supramolecular interaction, namely the lone pair···π interaction, has been considered to construct supramolecular framework [5], that is a type of noncovalent interaction between atoms that contain lone pair electron and electron-deficient π-ring [6]. Halogen bonding is also a "new" intermolecular interaction [7] that has attracted great interest in recent years [2,3,8–22]. It is an analogue of hydrogen bonding and is also used in crystal engineering to construct a variety of architectures [23–27]. The remarkable strength of some halogen bondings enable them to prevail over hydrogen bondings in the construction of crystal structures [28].

We are interested in searching for new intermolecular interactions to assemble supramolecules with novel structures [4,29–35]. The emergence of halogen bonding and lone pair···π interactions in recent years has motivated us to study their roles in the assembly of supramolecules. To evaluate the directional capacities of the N(sp^2)···Cl halogen bonding, lone pair···π interaction, C—H···O hydrogen bonding and π–π stack in the construction of supramolecules and to investigate the site selectivity of the N(sp^2)···Cl halogen bonding, we herein report the synthesis and crystal structure of two new azaaromatic chlorides (Scheme 1), bis-2,4-[(2-formoyl)phenoxyl]-6-chloro-[1,3,5]triazine (**1**) and bis-2,4-(4-carbomethoxyphenoxyl)-6-chloro-[1,3,5]triazine (**2**). The designs of the molecular structures **1** and **2** are based on the following considerations. First, azaaromatic chlorides may form short N···Cl contact in their solid state [36], which means the formation of strong halogen bonds [28]. Second, if a molecule has more than one N atom, it is possible that only some of them are involved in the formation of halogen bonding, which is a site-selective supramolecular synthesis [11]. Third, the lone pair···π interaction between carbonyl group and electron-deficient triazine ring could be used to assemble supramolecules [5].

An analysis of the crystal structures **1** and **2** reveals that N(sp^2)···Cl halogen bonding not only exists in the two crystal structures but also dominates the direction of self-assembly of the supramolecules. The formation of the N(sp^2)···Cl halogen bonding in these crystal structures is site-selective, as only the N atoms opposing to the C—Cl bonds (the opposing N atoms) on the molecules **1** and **2** are involved in the formation of the halogen bonding. In other words, the Cl atoms on the molecules **1** and **2** recognize the opposing N atoms. The lone pair···π interactions exist in the crystal structure of **1**. It is seldom reported that lone pair···π interactions and N···Cl halogen bonding take part in the assembly of supramolecules simultaneously.

To estimate quantitatively the capacity of halogen bonding, lone pair···π interaction, π–π stack and C—H···O hydrogen bonding in

---

[*] Corresponding author. Tel.: +86 20 84112977.
E-mail address: cesyyy@mail.sysu.edu.cn (Y.-Y. Yang).

0022-2860/$ - see front matter © 2010 Elsevier B.V. All rights reserved.
doi:10.1016/j.molstruc.2010.04.035

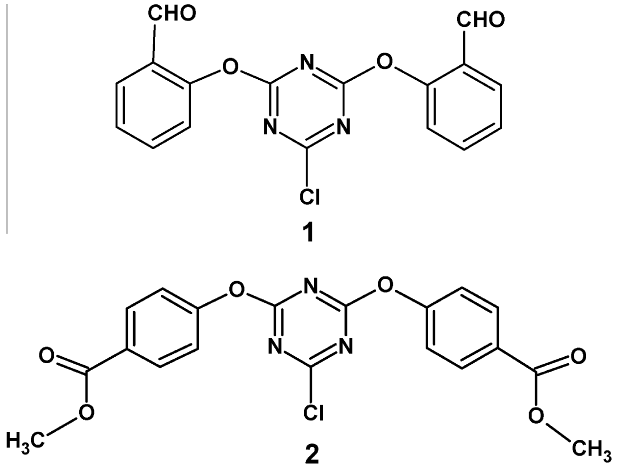

Scheme 1. Line drawings of the compounds **1** and **2**.

the direction of self-assembly of supramolecules, we calculated the strengths of the halogen bonding in these crystal structures, and compared the results with the strengths of the other three intermolecular interactions. We also calculated the molecular electrostatic potentials of **1** and **2**. The outcome may illustrate the site selectivity between Cl atoms and different N electron-donor sites on the triazine rings [13]. The results of the molecular electrostatic potential calculations indicate that the opposing N atoms in **1** and **2** have more abilities to interact with Cl atoms through the regions of negative potential on their surfaces. As a result, molecular electrostatic potential calculations have significant contribution in the description of the site selectivity between Cl atoms and different N electron-donor sites on the triazine rings. Additionally, this kind of site selectivity may partly contribute from the shape of the molecules, as suggested by Báthori et al. [36]. To the best of our knowledge, there are no reports on the study of the directionality of N(sp^2)···Cl halogen bonding and site selectivity of halogen bonding by using a structural method together with theoretical calculations.

2. Experimental

2.1. Synthesis

Both **1** and **2** were synthesized according to a literature procedure [37] with minor modifications.

2.1.1. Synthesis of bis-2,4-[(2-formoyl)phenoxyl]-6-chloro-[1,3,5]triazine (*1*)

2,4,6-Trichloro-1,3,5-triazine (10 mmol) was dissolved in THF (80 ml). Na_3PO_4 (20 mmol) was added and the suspension mixture was cooled to 0 °C. Salicylaldehyde (20 mmol) was added portionwise. After the completion of the addition, the suspension mixture was warmed to room temperature and then stirred at the same temperature for 8 h. The resulting mixture was filtered. To the filtrate was added water (400 ml) portionwise leading to the formation of a white precipitate. The precipitate was collected by filtration and washed with water (3 × 20 ml) and recrystallized from acetonitrile to give the white product **1**. Yield 1.43 g (40.2%); m.p. 207–208 °C. *Anal.* Calc. For $C_{17}H_{10}ClN_3O_4$ (**1**): C, 57.4; H, 2.8; N, 11.8; Found: C, 57.5; H, 3.0; N, 11.8%. FT-IR (KBr, cm^{-1}): 3082, 2765, 1698, 1606, 1560, 1358, 1273, 1234, 958, 770.

2.1.2. Synthesis of bis-2,4-(4-carbomethoxyphenoxyl)-6-chloro-[1,3,5]triazine (*2*)

2,4,6-Trichloro-1,3,5-triazine (10 mmol) was dissolved in THF (120 ml). K_2CO_3 (20 mmol) was added and the suspension mixture was cooled to 0 °C. Methyl p-hydroxybenzoate (20 mmol) was added portionwise. After the completion of the addition, the suspension mixture was warmed to room temperature and then heated at 50 °C for 6 h. The mixture was filtered and the solvent of the filtrate was evaporated under reduced pressure to give the crude product, which was recrystallized from THF to give the white powder **2**. Yield 2.41 g (49.4%); m.p. 201–202 °C. *Anal.* Calc. For $C_{23}H_{22}ClN_3O_7$ (**2**): C, 56.6; H, 4.5; N, 8.6; Found: C, 56.4; H, 4.4; N, 8.9%. FT-IR (KBr, cm^{-1}): 3007, 2957, 2848, 1723, 1561, 1529, 1365, 1283, 1242, 948, 773, 703.

2.2. X-ray crystallographic study

Colorless block crystals of 1 were grown from acetone in one week. Colorless plate crystals of 2 were grown from THF in a few days.

X-ray data were collected on a Bruker SMART 1000 CCD diffractometer, Mo Kα (λ = 0.71073 Å), graphite monochromator at T = 173(2) K (for **1**) and on an Oxford Gemini S Ultra diffractometer, Mo Kα (λ = 0.71073 Å), graphite monochromator at T = 150(2) K (for **2**). The initial structure models were obtained by direct methods [38] for **1** and by Patterson method [38] for **2** and subsequent difference synthesis for both **1** and **2**. H atoms were positioned geometrically and allowed to ride on their parent atoms with $U_{iso}(H) = 1.2U_{eq}(C)$ for CH and CH_2 groups and $U_{iso}(H) = 1.5U_{eq}(C)$ for CH_3 group. The structures were refined by full-matrix least-squares methods with SHELXL-97 module [39]. Crystallographic data are listed in Table 1.

2.3. Theoretical methods

All the calculations were preformed by means of the Gaussian03 program-package (revision D.01) [40]. All geometries were optimized in vacuo using the restricted DFT-B3LYP method and 6-311G* basis set. Based on the optimized geometries, the molecular electrostatic potentials were calculated at the same level of theory. The energies of the halogen bonding were calculated with

Table 1
Crystallographic data for **1** and **2**.

	1	2
Formula	$C_{17}H_{10}ClN_3O_4$	$C_{23}H_{22}ClNO_7$
Formula weight	355.73	487.89
Crystal system	Monoclinic	Orthorhombic
Space group	*C*2/*c*	*Pnma*
Crystal size (mm)	0.46 × 0.41 × 0.40	0.40 × 0.38 × 0.15
a (Å)	13.774(2)	7.4508(2)
b (Å)	7.460(1)	25.690(1)
c (Å)	15.246(3)	10.9543(4)
β (°)	99.489(3)	
V (Å^3)	1545.2(4)	2096.8(1)
Z	4	4
D_{calc} (g/cm^3)	1.529	1.546
μ (mm^{-1})	0.277	0.237
F(0 0 0)	728	1016
θ ranges (°)	3.00–27.07	3.31–27.99
hkl range	$-17 \leqslant h \leqslant 13$ $-8 \leqslant k \leqslant 9$ $-17 \leqslant l \leqslant 19$	$-9 \leqslant h \leqslant 4$ $-33 \leqslant k \leqslant 29$ $-14 \leqslant l \leqslant 13$
Reflections collected	4424	7096
Independent reflections	1689	2758
Observed reflections ($I > 2\sigma(I)$)	1473	1893
R_{int}	0.0164	0.0274
Goodness-of-fit on F^2	1.063	1.057
$R(F)$ ($I > 2\sigma(I)$)	0.0332	0.0682
$wR(F^2)$ ($I > 2\sigma(I)$)	0.0938	0.1918
$R(F)$ (all data)	0.0387	0.0944
$wR(F^2)$ (all data)	0.0987	0.2047
$\Delta\rho_{max}$, $\Delta\rho_{min}$ (e Å^{-3})	0.339 and −0.160	1.205 and −0.789

the DFT-B3LYP method and 6-311++G** basis set, using the same optimized geometries as mentioned above. In addition, to accurately obtain halogen bonding complexation energy, the basis set superposition error (BSSE) was taken into account using the counterpoise method [41].

3. Results and discussion

In the molecular structure of **1**, a twofold rotation axis passes through the C—Cl bond and the opposing N atom (Fig. 1). The two phenyl rings are almost perpendicular to the central triazine ring with the dihedral angles of 99.7° (phenyl ring C3—C8) and 80.3° (phenyl ring C3A—C8A), respectively. The two phenyl rings are more tilted towards each other (dihedral angle: 53.1°). **1** adopts the butterfly conformation with two torsion angles (N1—C2—O1—C3 and N1A—C2A—O1A—C3A) of 1.2(2)° [42]. Fig. 2 shows that each butterfly-shaped molecule in the crystal structure connects with two neighboring molecules in a head-to-tail mode through intermolecular N···Cl halogen bonding, affording an infinite one-dimensional supramolecular chain along the crystallographic *b* axis that is characterized by short N···Cl distances (3.095(2) Å) and linear C—Cl···N angles (180°). The N···Cl distance in **1** is much shorter than the sum of the effective van der Waals radii [36,43] (ca. 3.40 Å). The adjacent one-dimensional chains connect with each other through lone pair···π interaction [44] between electron-sufficient carbonyl O atoms and the electron-deficient triazine rings, giving rise to a two-dimensional supramolecular sheet (Fig. 2). The contact distances of the lone pair···π interaction are listed in Table 2. The two-dimensional sheets are linked by π–π stack between phenyl rings to form a three-dimensional supramolecular array (Fig. 3). The centroid–centroid distances within the stack are 3.8451(5) Å (measured in the Diamond program).

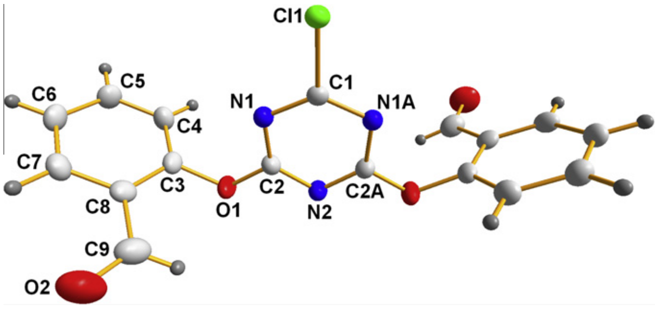

Fig. 1. An ORTEP diagram of the molecular structure of **1** showing the atom-numbering scheme and probability displacement ellipsoids drawn at the 50% level. Symmetry code: (A) −*x*, *y*, −*z* + 1/2.

In the molecular structure of **2**, a mirror plane bisects the triazine ring perpendicular to its plane across the C—Cl bond and the opposing N atom (Fig. 4). The molecules of **2** also adopt the butterfly configuration similar to that of **1**. Beside this, each molecule of **2** in stacks is also halogen bonded to two adjacent molecules in a head-to-tail mode, resulting in a one-dimensional chain (Fig. 5). The intermolecular distance between the N and Cl atoms forming the halogen bond is 3.088(3) Å and the angle of C—Cl···N is 177.6(2)°. However, the mode of packing of the one-dimensional chains in the crystal structure of **2** is quite different from that of **1**. In the crystal structure of **2**, two adjacent one-dimensional chains formed by halogen bonding connect with each other through intermolecular C—H···O hydrogen bonding that is involved in the methyl groups and the O atoms of the carbonyl groups to form a double-chain motif (Fig. 5, Table 3). Numerous double-chain motifs stack in a parallel mode to afford one-dimensional channels along the crystallographic *a* axis (Fig. 6). Disordered THF solvent molecules reside in these channels.

A comparison of the crystal structures of **1** and **2** showed that there are one-dimensional supramolecular chains formed by N···Cl halogen bonding and all the molecules in the same chain connect with one other in a head-to-tail mode in both the crystal structures of **1** and **2**. This phenomenon indicates that the Cl atoms are bonded to the opposing N atoms of the adjacent molecules selectively. These are site-selective supramolecular syntheses, since only the opposing N atoms are involved in the recognition processes.

Table 2
Characteristic contact distances (in Å) for lone pair···π interactions observed in the crystal structure of **1**[a].

N1···O2[b]	3.236(2)	C1···O2[b]	3.132(2)
N1[c]···O2[b]	3.181(2)	C2···O2[b]	3.267(2)
N2···O2[b]	3.319(2)	C2[c]···O2[b]	3.209(2)
Centroid···O2[b]	2.940(2)		

[a] The values in the table are measured in the diamond program.
[b] −*x*, −*y* + 1,−*z* + 1.
[c] −*x*, *y*, −*z* + 1/2.

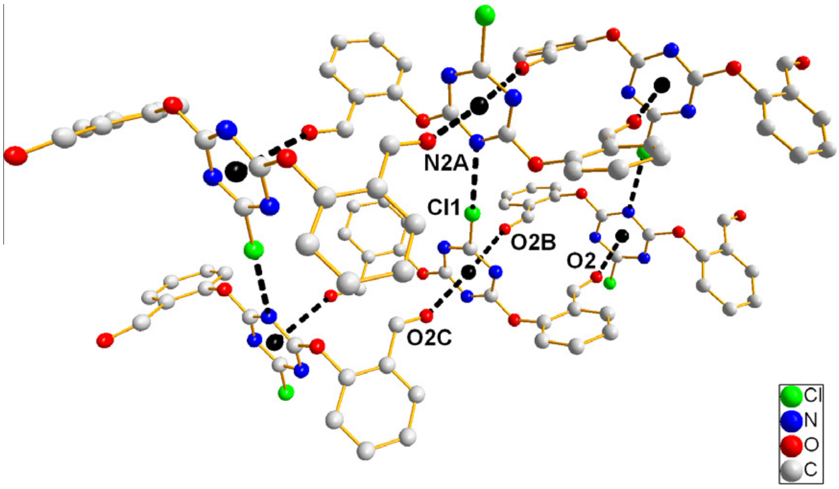

Fig. 2. Supramolecular interactions in the crystal structure of **1** showing the intermolecular N···Cl halogen bonding (in dashed lines) and lone pair···π interactions between O atoms on carbonyl groups and triazine rings (in dashed lines). H atoms have been removed for clarity. Symmetry codes: (A) *x*, *y* − 1, *z*; (B) *x*, −*y* + 1, *z* − 1/2; (C) −*x*, −*y* + 1, −*z* + 1.

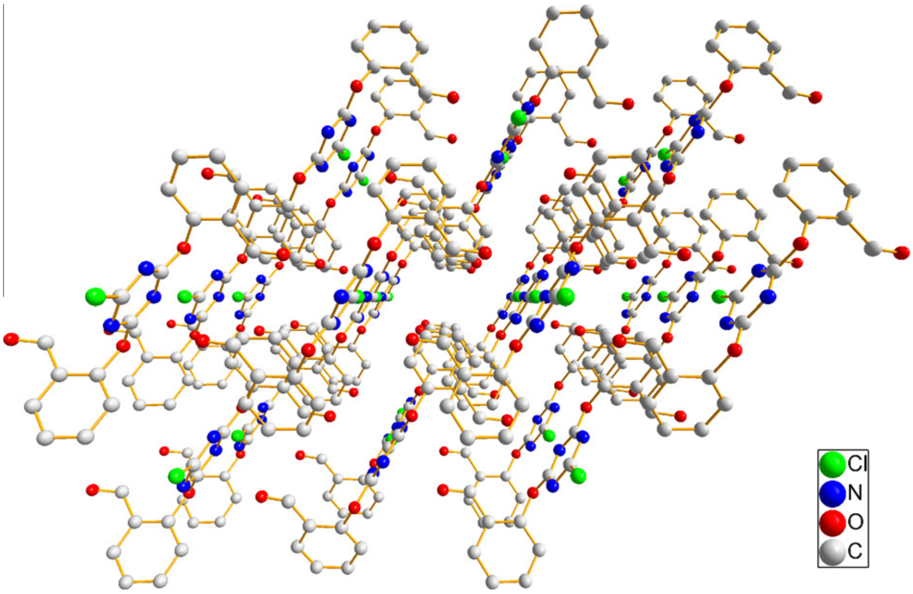

Fig. 3. Crystal packing of **1** showing π–π stack between benzene rings. H atoms have been removed for clarity.

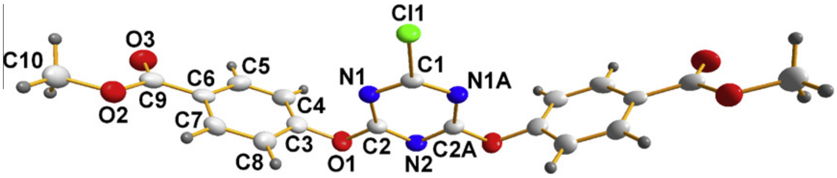

Fig. 4. An ORTEP diagram of the molecular structure of **2** showing the atom-numbering scheme and probability displacement ellipsoids drawn at the 50% level. Symmetry code: (A) x, $-y + 1/2$, z.

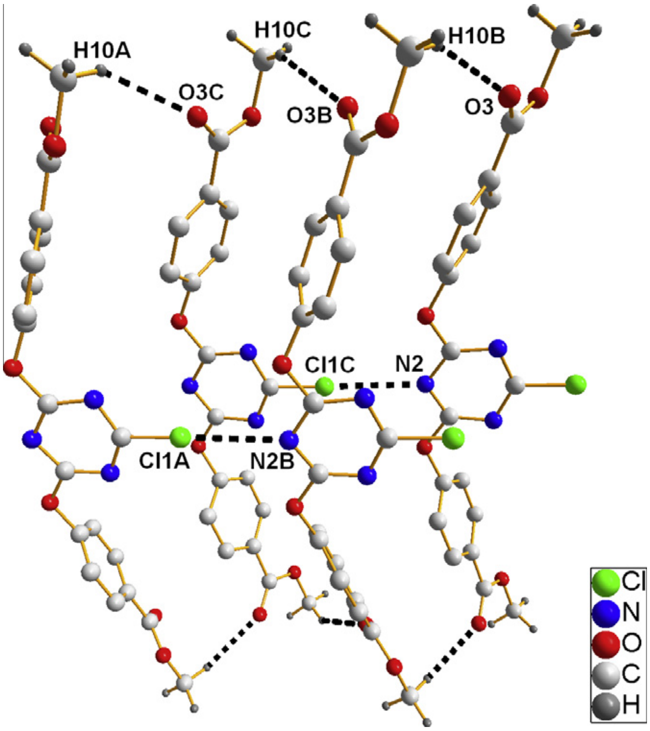

Fig. 5. A view of a double chain in **2** showing intermolecular N···Cl halogen bonding (in dashed lines) and intermolecular C–H···O hydrogen bonding (in dashed lines). H atoms of the phenyl rings have been removed for clarity. Symmetry codes: (A) $x - 3/2$, y, $-z + 3/2$; (B) $x - 1/2$, y, $-z + 3/2$; (C) $x-1$, y, z.

Table 3
Hydrogen bonding data of **2**[a] (distances in Å; angles in degree).

D–H···A	D–H	H···A	D···A	∠DHA
C10–H10C···O3[b]	0.980(3)	2.507(2)	3.343(4)	143.0(2)

[a] The values in the table are measured in the diamond program.
[b] $x-1/2$, y, $-z + 1/2$.

A calculation for the molecular electrostatic potentials of **1** and **2** shows that the site selectivity can be rationalized on the basis of a lower electrostatic potential of the opposing N atoms (−18.371 eV for **1** and −18.381 eV for **2**) than the adjacent N atoms (−18.366 eV for **1** and −18.375 eV for **2**). It means that the opposing N atoms are stronger electron donors than the adjacent ones. Figs. 7 and 8 show the molecular electrostatic potentials at the isodensity surface for **1** and **2**, respectively. It can be inferred from Figs. 7 and 8 that electrostatic interactions (N···Cl halogen bonding) can be formed selectively between the stronger electron donors (the opposing N atoms) and the regions of positive potential on the Cl atoms from the adjacent molecules. Shirman et al. [13] also reported that electrostatic potentials can be used as an effective tool for describing the capacity of molecules to interact through the regions of positive and negative potential on their surface.

There are obvious differences between the crystal structures **1** and **2**. First, there are other different intermolecular interactions besides halogen bonding in **1** and **2**, which are lone pair···π interaction between carbonyl O atoms and triazine rings and π–π stack between phenyl rings (for **1**), C–H···O hydrogen bonding between methyl groups and the O atoms of the carbonyl groups (for **2**).

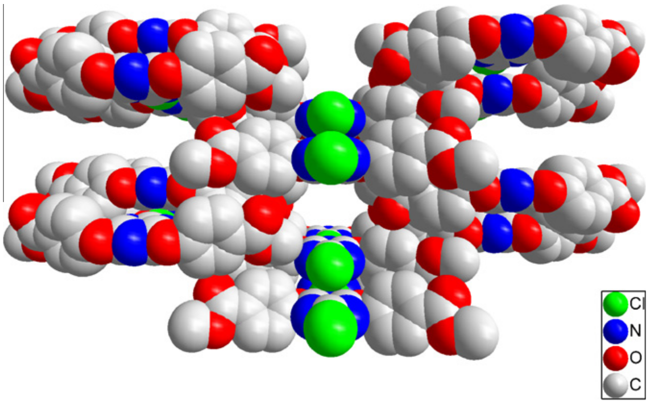

Fig. 6. Crystal packing of **2** viewed along the *a* axis that shows one-dimensional channels. Disordered THF solvent molecules in the channels and H atoms of the phenyl rings have been removed for clarity.

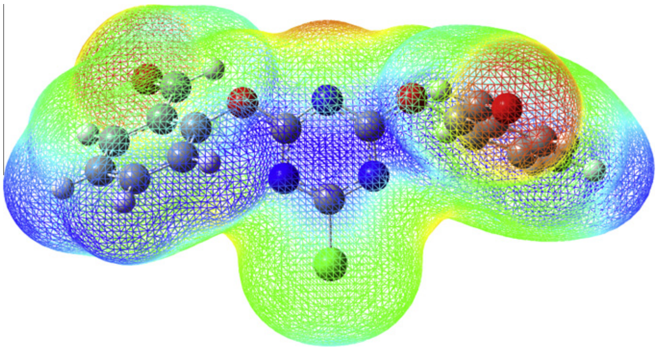

Fig. 7. The molecular electrostatic potential at the isodensity surface of **1**. Red indicates a value greater than or equal to the maximum in negative potential and blue indicates a value greater than or equal to the maximum in positive potential. (For interpretation of the references to colour in this figure legend, the reader is referred to the web version of this article.)

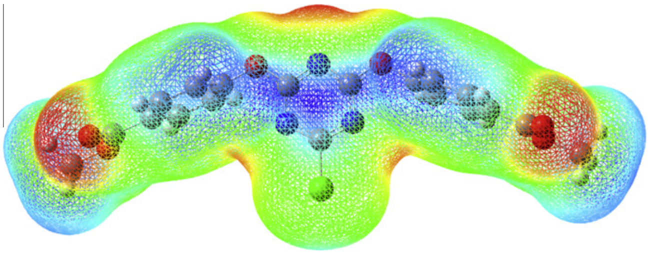

Fig. 8. The molecular electrostatic potential at the isodensity surface of **2**. Red indicates a value greater than or equal to the maximum in negative potential and blue indicates a value greater than or equal to the maximum in positive potential. (For interpretation of the references to colour in this figure legend, the reader is referred to the web version of this article.)

Second, the modes of packing of the chains formed by halogen bonding in the crystal structures **1** and **2** are also different. Based on the above results, it can be concluded that the N···Cl halogen bonding take the priority to direct the assembly of the crystal structures **1** and **2,** as there are the similar one-dimensional chains formed by N···Cl halogen bonding in both the case of **1** and **2** and that lone pair···π interaction, π–π stack and C–H···O hydrogen bonding are auxiliary forces which make the mode of packing of the one-dimensional chains formed by N···Cl halogen bonding different.

To develop a better evaluation for the capacity of N···Cl halogen bonding in the direction of the assembly of the crystal structures **1** and **2**, the strengths of the N···Cl halogen bonding in these crystal structures were further investigated from a theoretical perspective. The halogen bonding complexation energy of **1** and **2** in a gas-phase environment has been calculated as the following energy difference: $\Delta E_{\text{complex}} = E(\text{x} \cdot \text{x}) - 2E(\text{x})$ (1), where x stands for **1** or **2**. The $\Delta E_{\text{complex}}$ values yield −3.44 kcal/mol for **1** and −0.34 kcal/mol for **2**. The optimized intermolecular N···Cl distances are 3.098 and 3.270 Å for **1** and **2**, respectively. The optimized intermolecular N···Cl–C angles in **1** and **2** are 179.99° and 179.08°, respectively. These calculated distances are close to the values found in the crystal structures [45].

In the previous literature [46–50], the theoretical values of the strength of lone pair···π interaction are no less than −5.45 kcal/mol, the theoretical values of the strength of π–π stack between parallel displaced phenyl rings are −0.8 ~ −10.46 kcal/mol, and the experimental and theoretical values of the interaction energy of C–H···O hydrogen bonding are −0.77 ~ −2.72 kcal/mol. Consequently, the strengths of the N···Cl halogen bonding in the crystal structures **1** and **2** are comparable to those of lone pair···π interaction, π–π stack and C–H···O hydrogen bonding.

4. Conclusions

A study on crystal structures and DFT calculations shows that although the strengths of the N···Cl halogen bonding in the crystal structures **1** and **2** are comparable to those of lone pair···π interaction, π–π stack and C–H···O hydrogen bonding, the N···Cl halogen bonding has primary directionality in the construction of these crystal structures, leaving lone pair···π interaction, π–π stack and C–H···O hydrogen bonding as auxiliary forces. An analysis of the molecular electrostatic potentials of **1** and **2** reveals that the site selectivity of the N···Cl halogen bonding results from the lower electrostatic potential of the opposing N atoms than those of the adjacent ones. We may use halogen bonding and molecular electrostatic potential calculations to design, construct, and predict the structures of some supramolecules to some extent.

Acknowledgments

The authors acknowledge the financial support of National Natural Science Foundation of China (20973203) and Guangdong Natural Science Foundation (7003708).

Appendix A. Supplementary material

Crystallographic data for the structural analysis have been deposited with the Cambridge Crystallographic Data Centre, CCDC numbers 733851 and 733852. These data can be obtained free of charge via http://www.ccdc.cam.ac.uk/conts/retrieving.html (or from the Cambridge Crystallographic Data Centre, 12, Union Road, Cambridge CB2 1EZ, UK; fax:+44 1223 336033). Supplementary data associated with this article can be found, in the online version, at doi:10.1016/j.molstruc.2010.04.035.

References

[1] J.M. Lehn, Angew. Chem. Int. Ed. Eng. 27 (1988) 89.
[2] C.B. Aakeröy, N. Schultheiss, J. Desper, C. Moore, CrystEngComm 9 (2007) 421.
[3] M. Kubicki, J. Mol. Struct. 698 (2004) 67.
[4] W.-J. Lu, Y.-M. Zhu, K.-L. Zhong, Acta Crystallogr. C62 (2006) m448 (and references therein).
[5] C.Q. Wan, X.D. Chen, T.C.W. Mak, CrystEngComm 10 (2008) 475.
[6] C. Biswas, M.G.B. Drew, D. Escudero, A. Frontera, A. Ghosh, Eur. J. Inorg. Chem. 15 (2009) 2238.
[7] R. Rissanen, CrystEngComm 10 (2008) 1107.

[8] D. Hauchecorne, R. Szostak, W.A. Herrebout, B.J. van der Veken, ChemPhysChem 10 (2009) 2105.
[9] K.E. Riley, P. Hobza, J. Chem. Theory Comput. 4 (2008) 232.
[10] S. Triguero, R. Llusar, V. Polo, M. Fourmigué, Cryst. Growth Des. 8 (2008) 2241.
[11] D. Fox, P. Metrangolo, D. Pasini, T. Pilati, G. Resnati, G. Terraneo, CrystEngComm 10 (2008) 1132.
[12] A.C.B. Lucassen, A. Karton, G. Leitus, L.J.W. Shimon, J.M.L. Martin, M.E. van der Boom, Cryst. Growth Des. 7 (2007) 386.
[13] T. Shirman, J.-F. Lamere, L.J.W. Shimon, T. Gupta, J.M.L. Martin, M.E. van der Boom, Cryst. Growth Des. 8 (2008) 3066.
[14] G. Gattuso, A. Notti, S. Pappalardo, M.F. Parisi, T. Pilati, G. Resnati, G. Terraneo, CrystEngComm 11 (2009) 1204.
[15] M. Palusiak, S.J. Grabowski, Struct. Chem. 19 (2008) 5.
[16] S. Berski, Z. Ciunik, K. Drabent, Z. Latajka, J. Panek, J. Phys. Chem. B 108 (2004) 12327.
[17] Y.-X. Lu, J.-W. Zou, Y.-H. Wang, Y.-J. Jiang, Q.-S. Yu, J. Phys. Chem. A 111 (2007) 10781.
[18] N.J.M. Amezaga, S.C. Pamies, N.M. Peruchena, G.L. Sosa, J. Phys. Chem. A 114 (2010) 552.
[19] Y.-X. Lu, J.-W. Zou, J.-C. Fan, W.-N. Zhao, Y.-J. Jiang, Q.-S. Yu, J. Comput. Chem. 30 (2009) 725.
[20] T. Clark, M. Hennemann, J.S. Murray, P. Politzer, J. Mol. Model. 13 (2007) 291.
[21] P. Politzer, J.S. Murray, M.C. Concha, J. Mol. Model. 13 (2007) 643.
[22] P. Cauliez, V. Polo, T. Roisnel, R. Llusar, M. Fourmigué, CrystEngComm 12 (2010) 558.
[23] F.C. Pigge, V.R. Vangala, P.P. Kapadia, D.C. Swenson, N.P. Rath, Chem. Commun. 39 (2008) 4726.
[24] A.D. Santis, A. Forni, R. Liantonio, P. Metrangolo, T. Pilati, G. Resnati, Chem. Eur. J. 9 (2003) 3974.
[25] R. Liantonio, P. Metrangolo, F. Meyer, T. Pilati, W. Navarrini, G. Resnati, Chem. Commun. 17 (2006) 1819.
[26] P. Metrangolo, F. Meyer, T. Pilati, D.M. Proserpio, G. Resnati, Chem. Eur. J. 13 (2007) 5765.
[27] G.R. Hanson, P. Jensen, J. McMurtrie, L. Rintoul, A.S. Micallef, Chem. Eur. J. 15 (2009) 4156 (and references therein).
[28] P. Metrangolo, F. Meyer, T. Pilati, G. Resnati, G. Terraneo, Angew. Chem. Int. Ed. 47 (2008) 2 (and references therein).
[29] Y.-M. Zhu, P.-P. Feng, Y.-Y. Yang, S.W. Ng, Acta Crystallogr. E66 (2010) m54.
[30] Y. Cui, H.-J. Mo, J.-C. Chen, Y.-L. Niu, Y.-R. Zhong, K.-C. Zheng, B.-H. Ye, Inorg. Chem. 46 (2007) 6427.
[31] Y.-Y. Yang, Z.-Q. Huang, F. He, X.-M. Chen, S.W. Ng, Z. Anorg. Allg. Chem. 630 (2004) 286.
[32] Y.-Y. Yang, L. Szeto, W.-T. Wong, Appl. Organometal. Chem. 17 (2003) 958.
[33] Y.-Y. Yang, Z.-Q. Huang, L. Szeto, W.-T. Wong, Appl. Organometal. Chem. 18 (2004) 97.
[34] W.-J. Lu, Y.-M. Zhu, K.-L. Zhong, Acta Crystallogr. C63 (2007) m4.
[35] Y.-M. Zhu, K.-L. Zhong, W.-J. Lu, Acta Crystallogr. E62 (2006) m2688.
[36] N. Báthori, L. Bihátsi, P. Bombicz, M. Czugler, CrystEngComm 5 (2003) 42.
[37] P. de Hoog, P. Gamez, W.L. Driessen, J. Reedijk, Tetrahedron Lett. 43 (2002) 6783.
[38] G.M. Sheldrick, SHELXS-97, Program for Crystal Structure Solution, University of Göttingen, Germany, 1997.
[39] G.M. Sheldrick, Institüt für Anorganische Chemie der Universität, Tammanstrasse 4, D-3400, Göttingen, Germany, 1998.
[40] M.J. Frisch, G.W. Trucks, H.B. Schlegel, G.E. Scuseria, M.A. Robb, J.R. Cheeseman, J.A. Montgomery Jr., T. Vreven, K.N. Kudin, J.C. Burant, J.M. Millam, S.S. Iyengar, J.Tomasi, V. Barone, B. Mennucci, M. Cossi, G. Scalmani, N. Rega, G.A. Petersson, H. Nakatsuji, M. Hada, M. Ehara, K. Toyota, R. Fukuda, J. Hasegawa, M. Ishida, T. Nakajima, Y. Honda, O. Kitao, H. Nakai, M. Klene, X. Li, J.E. Knox, H.P. Hratchian, J.B. Cross, V. Bakken, C. Adamo, J. Jaramillo, R. Gomperts, R.E. Stratmann, O. Yazyev, A.J. Austin, R. Cammi, C. Pomelli, J.W. Ochterski, P.Y. Ayala, K. Morokuma, G.A. Voth, P. Salvador, J.J. Dannenberg, V.G. Zakrzewski, S. Dapprich, A.D. Daniels, M.C. Strain, O. Farkas, D.K. Malick, A.D. Rabuck, K. Raghavachari, J.B. Foresman, J.V. Ortiz, Q. Cui, A.G. Baboul, S. Clifford, J. Cioslowski, B.B. Stefanov, G. Liu, A. Liashenko, P. Piskorz, I. Komaromi, R.L. Martin, D.J. Fox, T. Keith, M.A. Al-Laham, C.Y. Peng, A. Nanayakkara, M. Challacombe, P.M.W. Gill, B. Johnson, W. Chen, M.W. Wong, C. Gonzalez, J.A. Pople, GAUSSIAN 03, Revision D.01, Gaussian, Inc., Wallingford, CT, 2005.
[41] S.F. Boys, F. Bernardi, Mol. Phys. 19 (1970) 553.
[42] N. Fridman, M. Kapon, Y. Sheynin, M. Kaftory, J. Incl. Phenom. Macro. Chem. 54 (2006) 153.
[43] R.S. Rowland, R. Taylor, J. Phys. Chem. 100 (1996) 7384.
[44] P. de Hoog, A. Robertazzi, I. Mutikainen, U. Turpeinen, P. Gamez, J. Reedijk, Eur. J. Inorg. Chem. 18 (2009) 2684.
[45] O.K. Poleshchuk, V. Branchadell, B. Brycki, A.V. Fateev, A.C. Legon, J. Mol. Struct. (Theochem.) 760 (2006) 175.
[46] A. Jain, V. Ramanathan, R. Sankararamakrishnan, Protein Sci. 18 (2009) 595.
[47] J. Ran, P. Hobza, J. Chem. Theory Comput. 5 (2009) 1180.
[48] Q. Li, N. Wang, Z. Yu, J. Mol. Struct. (Theochem.) 847 (2007) 68.
[49] Q. Li, X. An, F. Luan, W. Li, B. Gong, J. Cheng, J. Phys. Chem. A 112 (2008) 3985.
[50] B.W. Gung, J.C. Amicangelo, J. Org. Chem. 71 (2006) 9261.